ChemPubSoc Europe

DOI: 10.1002/slct.201600297

Chemistry SELECT Full Papers

Energy Technology & Environmental Science

Cobalt Sulfide as Counter Electrode in p-Type Dye-Sensitized Solar Cells

Mirko Congiu,*[a] Matteo Bonomo,*[b] Maria Letizia De Marco,*[b] Denis P. Dowling,*[c] Aldo Di Carlo,*[d] Danilo Dini,*[b] and Carlos F. O. Graeff*[a, e]

We proposed a novel application of cobalt sulfide (CoS) in the configuration of transparent thin film as anode in p-type dye-sensitized solar cell (p-DSC). The anodes here considered have been prepared using a water-based method that is suitable for the large scale production of large-area electrodes. The photoactive cathodes of the p-DSC were mesoporous nickel oxide (NiO) thin films deposited via rapid discharge sintering. The NiO electrodes were sensitized with the benchmark dye erythrosine B (ERY), while the couple I^-/I_3^- was the redox mediator. The CoS anodes showed higher electrocatalytic efficiency in comparison with the commonly used platinized Fluorine-doped Tin Oxide (Pt-FTO). This was determined by means of electrochemical impedance spectroscopy of CoS based dummy cells, with CoS showing a lower charge-transfer resistance with respect to Pt-FTO. The overall conversion efficiency of the p-DSC employing ERY-sensitized NiO as photoactive cathode and CoS anode was 0.026%, a value very close to that obtained with Pt-FTO anodes (0.030%). The external quantum efficiency spectra of the p-DSCs with CoS anodes were similar to those obtained with Pt-FTO anodes under illumination with AM 1.5 solar simulator.

Introduction

Solar energy represents by far the most important source of renewable energy and the sole convincing alternative to fossil fuels for the production of electrical energy without any secondary production of carbon dioxide. For this reason, many efforts have been done by the scientific community to discover and improve new technologies for renewable energy production within the context of photovoltaics. Within the framework of solar energy conversion technologies and devices, the dye sensitized solar cell (DSC)[1] constitutes one of the most important developments after the pioneering advent of silicon based *pn* junctions. DSC can be considered an organic cell since it utilizes an organic (or organometallic) dye as main photoactive component. The latter is anchored to the surface of a metal oxide semiconductor (e.g. TiO_2, ZnO or NiO) with nanostrucrtured morphology and it is generally responsible for light harvesting in the visible and near UV spectrum. When DSC appeared for the first time as a solar conversion device with superior performance, in 1991 O'Regan *et al.* reported on DSCs capable to produce efficiencies up to 8% utilizing a ruthenium-based complex as sensitizer to be anchored to a mesoporous TiO_2 sintered layer.[2] More recently the same type of solar conversion device reached efficiencies up to 13% using a porphyrine sensitizer on mesoporous TiO_2 when Co(II)/(III) was the redox mediator.[1] Recent research on *n*-type DSCs involved also the use of ZnO as alternative *n*-type semiconductor but the results were not as promising as those obtained with the photoelectrochemical cells employing TiO_2 photoanodes.[3] In *n*-type DSCs, the electron of the HOMO of the dye is excited to the LUMO level and then injected into the conduction band of the *n*-type semiconductor. The injected electron is collected at the external contact after diffusing in the sensitized nanostructured metal oxide. The as oxidized dye is regenerated by the redox mediator with the mediator which, in turn, will be regenerated at the cathode. On the contrary, in a *p*-type DSC the electron promoted from HOMO to LUMO upon light absorption of the dye is transferred directly to the redox mediator. The oxidized dye is thus regenerated by the oxide substrate through hole injection into the valence band (VB) of the *p*-type semiconductor (generally made of NiO).[4] The reduced redox mediator is then regenerated at the counter electrode (CE). Basically a general DSC is composed by 5 elements: a transparent conductive layer (TCO), a dye, a mesoporous semiconducting film

[a] *Dr. M. Congiu, Prof. C. F. O. Graeff*
UNESP – Univ. Estadual Paulista, POSMAT - Programa de Pós-Graduação em Ciência e Tecnologia de Materiais, Av. Eng. Luiz Edmundo Carrijo Coube14-01, 17033-360 Bauru, SP, Brazil.
E-mail: mirko.congiu@fc.unesp.br
graeff@fc.unesp.br
[b] *Dr. M. Bonomo, Dr. M. L. D. Marco, Prof. D. Dini*
University of Rome ''La Sapienza'', Department of Chemistry, Piazzale Aldo Moro 5, Rome, RM, Italy
E-mail: matteo.bonomo@uniroma1.it
mletizia.demarco@gmail.com
danilo.dini@uniroma1.it
[c] *Prof. D. P. Dowling*
University College Dublin, UCD, Belfield, Dublin 4, Ireland
E-mail: denis.dowling@udc.ie
[d] *Prof. A. D. Carlo*
C.H.O.S.E.-Center for hybrid and organic solar energy, Department of Electrical Engineering, University of Roma "Tor Vergata", via del Politecnico 1, 00133, Rome Italy
E-mail: aldo.dicarlo@uniroma2.it
[e] *Prof. C. F. O. Graeff*
DC-FC - UNESP – Univ. Estadual Paulista, Av. Eng. Luiz Edmundo Carrijo Coube14-01, 17033-360 Bauru, SP, Brazil

Supporting information for this article is available on the WWW under http://dx.doi.org/10.1002/slct.201600297

(either *p*-type NiO or *n*-type TiO_2), an I^-/I_3^- based electrolyte and a catalytically active CE. In order to obtain a performing solar cell, all components need to be properly assembled by means of appropriate procedures including dying of the mesoporous films and electrolyte definition/preparation. The quality of starting materials and the performance of each single component are also strongly influencing the efficiency of DSCs. The counter electrode (CE) is a fundamental part of a DSC device since it is responsible for the regeneration of the redox couple and allows the continuous cycling of the device. In the case of *n*-type solar cells, the CE transfers an electron to the oxidized form of the redox mediator whereas in *p*-type DSCs the CE gives rise to the oxidation of the reduced form of the mediator. In a standard DSC either of *n*- or *p*-type, the CE consists of a thin layer of electrocatalytically active platinum nanoparticles deposited by sputtering,[5] screen-printing[6] or electrodeposition[7] onto a TCO. However, Pt is a rare and expensive metal and its employment in DSCs increases noticeably the overall costs of the devices production. In order to reduce the costs of CEs several alternative materials have been proposed so far in the literature. These include graphene,[8] carbon nanotubes,[9] metallic PEDOT[10] and transition metal sulphides.[11] The more promising class of alternative materials is represented by metal sulphides, due to its low production cost, great availability, high stability and durability.[11–13] Different metal sulphides have been proposed as cathodes in *n*-type DSC such as Ni_2S_3, Co_2S_3, CoS_2 and $Cu_{2-x}S$.[14–16] As reported by us in 2015, thin transparent CoS films have shown high efficiency and stability also using a ferrocene-based liquid electrolyte (FCE) instead of the largely used I_3^-/I^- which possesses corrosive properties. Furthermore such electrodes were prepared using water-based solutions of starting materials that were cheap and suitable for large scale production since their disposal would have a very low environmental impact.[13] Cobalt sulfide (CoS) films can be obtained through several chemical or electrochemical processes such as electrodeposition, chemical vapor deposition and ink-based methods. CoS electrodes have shown an electrocatalytic effect in the process of I_3^- reduction in comparison to platinized TCOs in *n*-type DSC.[12,17–19] However, so far in the literature, we have not noticed any application-specific study of CoS in *p*-type cells probably because of the prevention caused by the fact that CoS is a *p*-type semiconductor in itself. In the present work, we consider the utilization of CoS thin films as anodes to be coupled with NiO photocathodes sensitized with erythrosine B (ERY) in *p*-type DSCs employing the redox mediator I^-/I_3^-. It will be here demonstrated for the first time that CoS is a suitable material as anode of a *p*-type DSC when NiO is the photoactive cathode and I_3^-/I^- is the redox shuttle.

Results and Discussion

Optical and electrochemical characterization of CEs

Prior to their employment as anodes in *p*-DSC devices, the CoS CEs have been characterized with electrochemical and optical methods. In order to obtain a good performance in the final *p*-DSC, CEs have to fulfill several requirements: (i) they should possess thermal and electrochemical stability; (ii) show a reversible behavior toward any redox process that must occur at the CE; (iii) warrant the flow of the charge through their structure with a minimal electrical resistance.

First of all, we conducted a compared optical analysis of CoS and Pt-based CEs. Pt-CE showed a slightly higher transmittance compared to CoS-CE. The FTO (substrates contribution) transmittance spectrum was subtracted from the spectra of the samples. In Figure 1 the optical transmission spectra of Pt and a CoS thin films on FTO are shown.

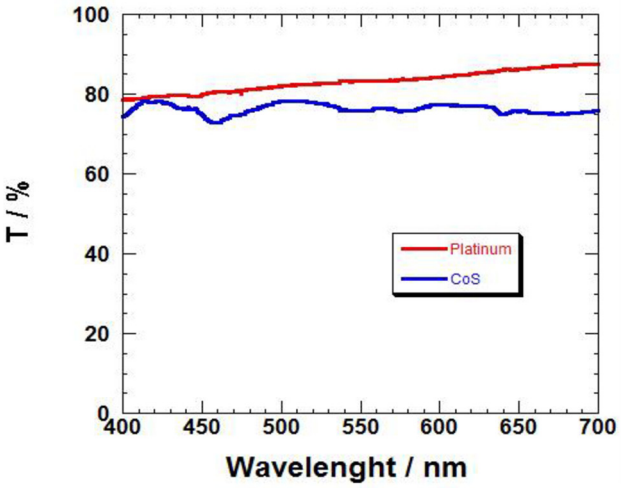

Figure 1. Transmittance spectra of CoS CE (blue line) and Pt-FTO CE (red line). The profiles here shown were obtained after subtraction of the FTO contribution (blank: bare FTO in air).

In the range 550–700, CoS resulted at least 10% less transparent than Pt as shown in Figure 1. However, the transmittance in the range 400–550 nm is quite similar for CoS and conventional Pt-based CE. Notice that the visible light absorption band of the considered dye (ERY) is located between 480 and 560 nm with a peak at 524 nm (see supporting information (S.I.), Figure S1). This aspect is particularly relevant if one considers that a CE, transparent in the absorption region of the dye, allows the efficacious illumination of the cell from both cell sides thus increasing the quantity of direct or diffuse light reaching the photoactive electrode. Successively, the electrochemical properties of *p*-DSC CEs were evaluated with a three electrode cell through cyclic voltammetry and electrochemical impedance spectroscopy (EIS) (Figure 2) in order to understand the characteristics of the charge transfer process at the CE/electrolyte interface.

In the comparative analysis of the electrochemical behavior of CoS and Pt nano islands a particularly important parameter must be determined: the charge transfer resistance (R_{ct}) associated to the electrocatalytic efficiency of the CE. The lower the R_{ct} the most efficacious will result the electrocatalytic effect of the CE. From the voltammograms of Figure 2 (left plots) it results that CoS and Pt CEs showed a similar current/voltage response in dummy cells using I^-/I_3^- as redox shuttle (electrolyte:

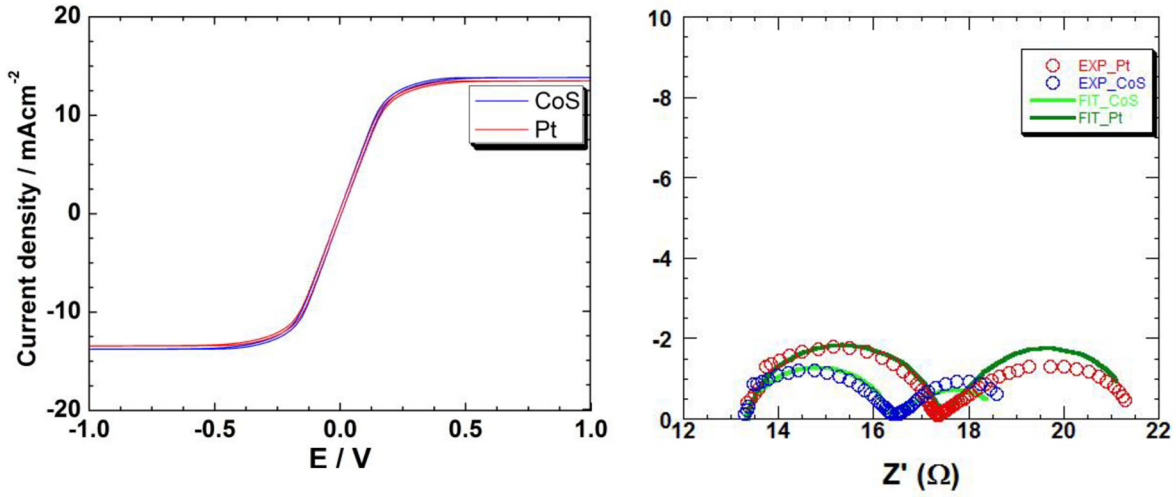

Figure 2. Left: cyclic voltammetry (CV) responses of CoS-CE (blue) and Pt-CE (red) dummy cells. Right: corresponding electrochemical impedance spectra of the dummy cells with CoS-CE (blue) and Pt-CE (red) electrodes. In the right plot the green line represents the fit obtained with the equivalent circuit of Figure 3 (*vide infra*). Both CV and EIS measurements were carried out in dark conditions, using two identical electrodes (WE═CE) in the case of dummy cells while in the measurements performed on complete DSCs the photochatode was considered as WE and CoS or Pt as CEs. In both the configurations, the iodine-based electrolyte was BV12-HSE (Dyers).

High Stability Electrolyte (HSE)). It must be noted that the slope of the voltammograms represents a resistive term that can be correlated to the efficiency of the electrode. In fact, the straight part of the voltammogram represents a linear ohmic response. In this portion of the voltammogram the slope of the two curves is inversely proportional to the sum of all the resistive elements of the system, according to the Ohm's law. Beside electrolyte resistance, the term R_s (for its meaning *vide infra*) depends also on the external resistance of the electrical contact between the substrate (FTO) and the active layer (Pt nanoislands or CoS). At the extremes of the linear portion the voltammogram becomes horizontal with the current reaching a constant value (*plateau*). Such a value of limiting current depends on the concentration of the redox active species in the electrolyte, and on its diffusion coefficient according to the equation of Cottrell.[20] In fact, the maximum current that can flow through the device is limited by the concentration of the ions in the electrolyte (I^-/I_3^-). The values of limiting current were 13.47 and 13.87 mA/cm^2 for Pt nanoislands and CoS, respectively. The Randles equivalent circuit (Figure 3) has been taken as circuit model to fit the EIS profiles (Figure 2, right plots) of the dummy cells using separately the CEs under investigation. Besides R_{ct}, the Randles circuit includes two other resistances: the series resistance (R_s) of the various ohmic contacts and ohmic elements in the cell, and the resistance contained in the Warburg diffusion element W_s. In order to calculate R_s; the double layer capacitance (C_{dl}) and the diffusion impedance (Z_d) associated to the Warburg element (Figure 3) the EIS profiles of the dummy cells (Figure 2, right graphs) were fitted using the *Z*-view software (see Experimental Section). The high frequency semicircle referred to CoS CEs resulted smaller than that of Pt nanoislands. The fitting values of R_{ct} for CoS and Pt CEs were 1.51 and 2.30 Ω cm^2 respectively. The lower value of R_{ct} for CoS indicates the higher electrocatalytic efficiency of CoS with respect to platinized FTO.

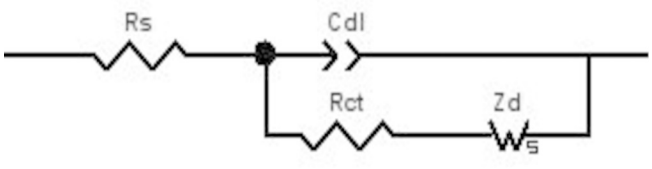

Figure 3. Randles equivalent circuit used to fit the EIS spectra and calculate the charge transfer resistance (R_{ct}); the series resistance (R_s); the double layer capacitance (C_{dl}) and the impedance (Z_d) associated to the Warburg diffusion element (W_s).

The double layer capacitance C_{dl} associated to the charge distribution at the CE/electrolyte interface is different for the two different CEs: 13.01 and 40.09 μF cm^{-2} for CoS and platinized FTO, respectively. The second semicircle of the impedance spectra at lower frequencies is associated to diffusion phenomena of the redox species in the electrolyte and will not be further discussed.

Morphological characterization of mesoporous NiO

The sintering time required in the rapid discharge sintering (RDS) procedure is much shorter than sintering with conventional furnace, and for this reason films sintered by RDS exhibit a finer crystallite structure as well as a larger surface area compared to electrodes treated by furnace. These characteristics allow a higher quantity of dye to be adsorbed on the electrode's surface, the consequent increase of the photocurrent density generated and the overall conversion efficiency.[21,22] The XRD

analysis showed that the films are composed by small crystallites of cubic NiO of about 7.5 nm, as calculated with the Scherrer equation.

Both XRD pattern (Figure 4) and optical profilometry graph (Figure 5) pointed out the mesoporous morphology of these

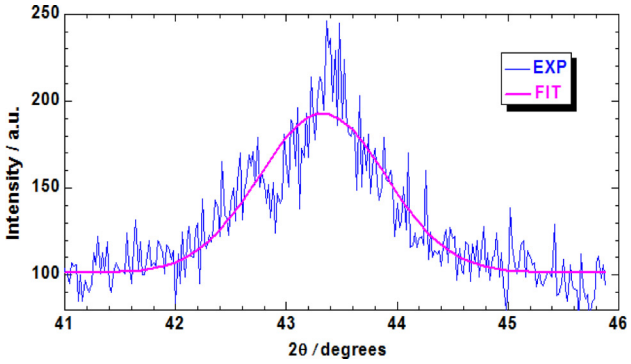

Figure 4. Diffraction peak corresponding to the reflection of the (200) crystallographic planes of nanocrystalline NiO; experimental data are shown in blue while the Gaussian fit is shown in pink colour.

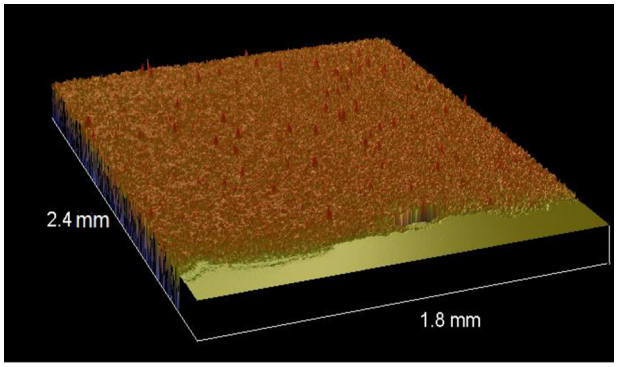

Figure 5. Top: surface imaging of nanocrystalline NiO film in 3D. bottom: determination of the thickness with optical profilometry.

NiO layers which are characterized by a surface roughness, R_a, of about 800 nm. Since the NiO films are porous, increasing the thickness causes the increase of the surface area, and consequently of the quantity of dye which is possible to load on the electrodes. On the other side, because of NiO dark color, too thick film will result to absorb too much light, preventing radiation from reaching the inner part of the electrode, and thus affecting the overall conversion efficiency of the *p*-type photoelectrochemical device. We decided to set the thickness of the NiO cathodes between 2.0 and 2.5 µm: this narrow range, from previous works,[21,22] resulted the optimum for this kind of electrodes.

Photoelectrochemical characterization of NiO based p-DSCs

Complete assembled cells were first characterized by recording the current voltage (JV) characteristic curves under illumination and in dark conditions (Figure 6) to determine the overall conversion efficiency. The overall efficiency of the *p*-DSC devices

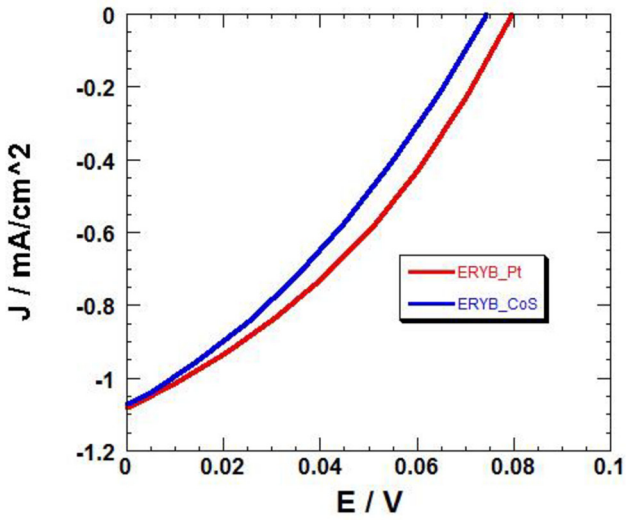

Figure 6. *JV* curves of the complete *p*-DSC employing CoS (blue) or platinized FTO (red) as CEs recorded (top) under illumination and (bottom) in dark conditions.

using the platinized CE was slightly higher compared to that of CoS CEs cells. Such a trend was mainly due to higher values of open-circuit-voltage (V_{OC}) and fill factor (FF) recorded for the *p*-DSC with the Pt-based CE (Table 1). In theory the V_{OC} parameter

Table 1. Photovoltaic parameters obtained from the *JV* curves registered from 0 to 0.1 V under simulated sun light (AM 1.5). Open circuit voltage (V_{oc}); short circuit current (J_{sc}); fill factor (FF) and overall energy conversion efficiency (η) are reported.

p-DSC configuration	V_{OC} / mV	J_{SC} /mA cm^{-2}	FF / %	η / %
NiO/ERYB/Pt-FTO	80	-1.059	34.8	0.030
NiO/ERYB/CoS	74	-1.051	32.5	0.026

of a DSC is affected by the relative positioning of the VB upper edge of the oxide semiconductor (i.e. NiO), and the redox potential level of the shuttle (i.e. I^-/I_3^-). The difference here reported could be due to a chemical reaction occurring between CoS counter electrode and the redox shuttle which consumes either the oxidized or reduced form of the redox mediator at a different extent. This chemical process would bring about the consequent alteration of the redox potential level of the I^-/I_3^- couple as defined by the Nernst equation,[23] due to a change of the concentration ratio $[I^-]/[I_3^-]$ at CoS surface. Such a consideration would explain straightforwardly the behavior observed with CoS.

The overall efficiency of the *p*-DSC devices using the platinized CE was slightly higher compared to that of CoS CEs cells. Such a trend was mainly due to higher values of V_{OC} and FF recorded for the *p*-DSC with the Pt-based CE (Table 1). In theory

the V_{OC} parameter of a DSC is affected by the relative positioning of the VB upper edge of the oxide semiconductor (i.e. NiO), and the redox potential level of the shuttle (i.e. I^-/I_3^-). The difference here reported could be due to a chemical reaction occurring between CoS counter electrode and the redox shuttle which consumes either the oxidized or reduced form of the redox mediator at a different extent. This chemical process would bring about the consequent alteration of the redox potential level of the I^-/I_3^- couple as defined by the Nernst equation,[23] due to a change of the concentration ratio $[I^-]/[I_3^-]$ at CoS surface. Such a consideration would explain straightforwardly the behavior observed with CoS. Nevertheless, as reported in dark CV measurements (Figure 2, left plot), no evidence of CoS CE degradation could be noticed. Another difference between Pt and CoS CEs is evidenced by the JV measurements performed in dark conditions (Figure 6, bottom plot). CoS shown a lower dark current in comparison with Pt. This can be addicted to the effect of CoS CE on the hole transport properties of NiO. In fact, as confirmed by impedance spectroscopy (Figure 8 and Table 3), the p-type nature of CoS CE influences the recombination kinetics at the interface NiO//electrolyte (see S.I., Tables S1 and S2). Different to *p*-type, *n*-type DSCs showed no significant alterations in *Voc* nor degradation phenomena as demonstrated in recent studies reporting the use of CoS as cathodic counter electrode.[11–13,17,18] These reactions could be probably ascribed to the working conditions adopted for CoS CEs in a *p*-type device. Since CoS is intrinsically a *p*-type semiconductor, in a *p*-type DSC it will be forced to operate as an anode. In such conditions, CoS will result generally reverse-biased (RB) when the cell is exposed to light. Adverse reactions in RB conditions have been recently reported in previous studies of *n*-type DSC when I^-/I_3^- as redox mediator.[24–26] However, the observed little differences in V_{oc} do not affect significantly the overall efficiency of the two differently configured *p*-DSCs (Table 1).

Expectedly, the incident photon-to-electron conversion efficiency (IPCE) spectra of the two *p*-DSCs differing for the sole CE presented the same profile (Figure 7) with the display of two main broad peaks: the peak comprised in the wavelength range 350–420 nm (which is due to the photoelectrochemical activity of bare NiO[27]); the doubly peaked large absorption in the spectral region 450–550 nm associated to the photoelectrochemical activity imparted by the absorption of ERY sensitizer.[22,28] The small differences in the IPCE peak values are ascribable to the analogously small differences in optical transmission for the two types of *p*-DSCs (Table 2).

Therefore, we concluded that the employment of CoS as a cheaper and valid alternative to platinized-FTO in the role of CE of a NiO based *p*-DSC is feasible since *p*-DSCs with CoS CEs reach practically the same overall cell efficiency of those using Pt-FTO. The EIS characterization was performed on assembled *p*-DSCs differing solely for the nature of the CE (Figure 8) to evaluate quantitatively the effect of the different CEs on the electrochemical parameters determinable through the definition of an appropriate equivalent circuit model fitting the EIS profiles. The latter were determined when the two different types of *p*-DSCs were kept in both dark and illuminated conditions. Impedance measurements were conducted at the value of open circuit potential (see Figure 6 and Table 1). The analysis of the impedance spectra generated by the NiO based *p*-DSCs

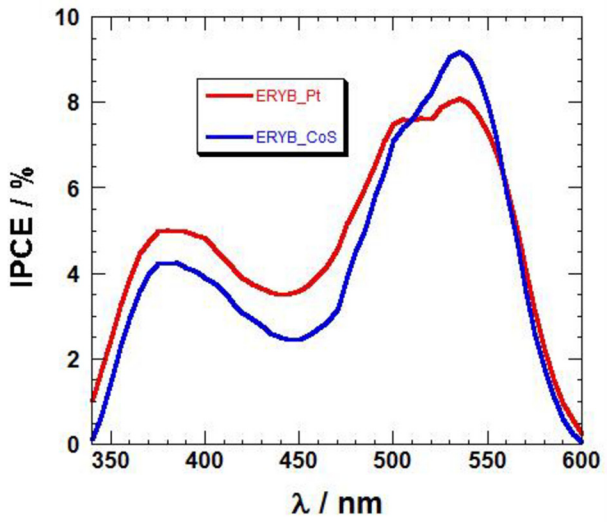

Figure 7. IPCE spectra of Pt-FTO based *p*-DSC (red) and CoS based *p*-DSC (blue) with the same photoelectroactive cathode of RDS NiO.

Table 2. Wavelengths of the two main IPCE maxima (Figure 7),and optical transmittance values of assembled devices in correspondence of these wavelengths.

	NiO/ERY/Pt	NiO/ERY/CoS
λ_1 / nm (T /%)	385 (5.00)	385 (4.25)
λ_2 / nm (T /%)	535 (8.10)	535 (9.19)

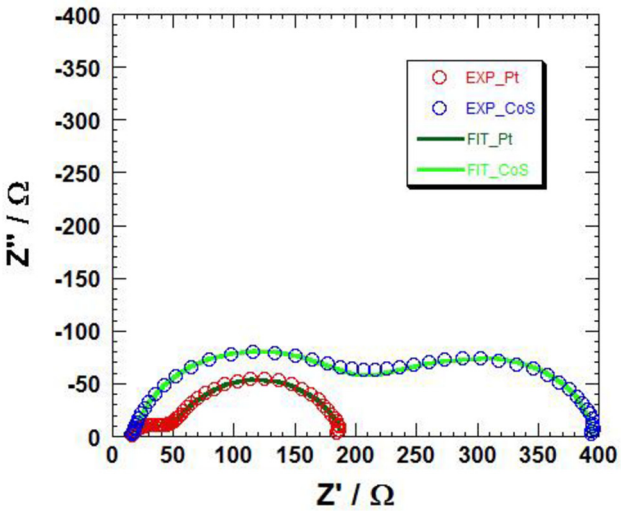

Figure 8. Top: EIS spectra of the p-DSCs differing for the CE when the cell was polarized at V_{OC} (see Table 1) and illuminated with 1 sun. Bottom: corresponding EIS profiles of the same cells at open circuit potential (see Figure 6 in dark conditions. The inset in the bottom plot reports the dark EI spectra zoomed in the high frequency region. Empty dots indicate experimental data (CoS in blue, Pt-FTO in red) whereas green solid lines represented the fitting curves.

under investigation has been conducted utilizing the approach first employed by Bisquert[29] for the analysis of the electrochemical impedance spectra of TiO_2-based *n*-DSC.

In Figure 9 it is shown the equivalent circuit we have adopted to model the experimental EIS profiles of Figure 8. For the

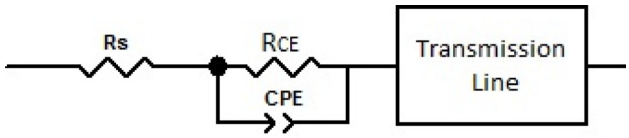

Figure 9. Equivalent circuit used to fit the experimental data of impedance for the complete *p*-DSC devices under artificial solar light and in dark conditions. *Rs* represents the series resistance (*vide supra*), R_{CE} is the charge transfer resistance at the interface counter electrode/electrolyte, CPE is the constant phase element linked to the charge distribution at the double layer generated at the counter electrode/electrolyte interface with prevalently capacitive character. The transmission line is an element that considers the electrochemical behavior of the porous film of RDS NiO, i.e. the *p*-type semiconductor.

calculation of the relevant kinetic parameters related to the fitting values of the circuital elements (*vide infra*) we have taken into account the different nature of the photoinjected charge carriers in *p*-DSC with respect to *n*-DSC, i.e. holes instead of electrons.

The equivalent circuit presented in Figure 9 for the analysis of *p*-DSC impedance spectra consists in: (i) a series resistance element associated to the ohmic transport through the external circuit of device (R_s, see Figure 3); (ii) the resistance term R_{CE} in parallel with the capacitive term CPE, i.e. the constant phase element, representing the phenomena occurring at the CE/electrolyte interface; (iii) a transmission line element modeling the behavior of the porous NiO film at the interface with the electrolyte, which takes also into account the internal charge transport through the mesoporous film of NiO. Some key parameters related to the charge transport properties of the NiO film can be directly obtained from the interpolation process: the most important ones are the hole transport resistance (R_t) through NiO film, and the charge transfer resistance R_{rec} through the NiO-ERY/electrolyte interface at the condition of open circuit potential, which is also described as recombination resistance. Moreover, the chemical capacitance C_μ included in the transmission line (Figure 9) can be straightforwardly deducted from the fitting value of CPE through the relationship $C_\mu = (C_{CPE}{*}R_{rec})^{1/n}/ R_{rec}$ where both C_{CPE} and *n* are fitting parameters.[30,31] Other parameters directly related to the terms present in the definition of the transmission line are: the hole diffusion time τ_d ($= R_{t*}C_\mu$), i.e. the transit time spent by the photoinjected charge carrier to cross the semiconducting layer (parameter of charge transport characteristic of the DSC in non-open circuit condition); the recombination time τ_h ($= R_{rec*}C_\mu$), i.e. the lifetime of the photoinjected hole before it undergoes recombination phenomena (this DSC parameter is characteristic of the open circuit condition); the diffusion coefficient D_h ($= L^2/ \tau_d$) of the photoinjected hole in the NiO layer with nominal thickness *L*; the diffusion length L_h [$= L{*}(R_{rec}/R_t)^{0.5}$] i.e. the distance the photoinjected hole travels by diffusion within the *p*-type semiconductor layer. As far as the CE of the *p*-DSC is concerned, its characterization and performance evaluation relies on the determination of the term R_{CE}, i.e. the charge transfer resistance at the CE/electrolyte interface, and of the term C_{CE} describing the capacitance of the double layer generated at the CE/electrolyte interface. A more in-depth electrochemical characterization and the calculation of the key transport parameters are provided in the S.I. (section S2).

The charge transfer resistance of the CE is generally higher in passing from the illuminated to the dark state. This is expectable since the arrival of a larger number of holes in the CE from the external circuit, and the presence of a larger concentration of the reduced form of the redox mediator at the CE/electrolyte interface as a consequence of the light induced injection of holes in ERY-sensitized NiO, favors the bimolecular anodic process of iodide oxidation at the CE. When the *p*-DSC is in the illuminated state the R_{CE} of the Pt-based counter electrode (Table 3) is lower than that of CoS due mainly to the *p*-type

Table 3. CE characteristic terms obtained by fitting the experimental data of Figure 8 with the model of equivalent circuit depicted in Figure 9. R_{CE} and C_{CE} are the resistive and capacitive terms associated respectively to the charge transfer resistance and the double layer capacitance at the CE/electrolyte interface

CE	cell state	R_{CE} / Ω	C_{CE} / μF
Pt-FTO	illuminated	16.90 ± 0.14	2.82 ± 0.06
CoS	illuminated	156.2 ± 3.8	1.42 ± 0.10
Pt-FTO	dark	33.3 ± 0.4	3.03 ± 0.12
CoS	dark	1035 ± 17	1.61 ± 0.08

semiconducting nature of the latter material. Such an experimental evidence could be explained with a higher number of photoelectrons reaching the CE to warrant continuity of charge transport through the external electronic circuit in case of Pt-based CE in comparison to CoS. Associated with the lower resistance there is correspondingly the larger value of the double layer capacitance since the less resistive CE material will afford an accumulation as well as the passage of a larger amount of charge carriers. The difference of capacitance at the CE can be at the basis of the observed decrease of the open circuit potential of the *p*-DSCs in passing from the Pt-based CE material to CoS CE (Table 1). The *JV* curves (Figure 6, top plot) and IPCE data (Figure 7) prove that *p*-type CoS is capable to catalyze also the oxidation of I^- upon neutralization of CoS holes in the VB. The holes present in the VB of CoS have been partly introduced by the process of the NiO-ERY hole photoinjection through the external circuit. This is equivalent to say that the electrochemical process of iodide oxidation at CoS CE is supposed to be based on the transfer of the majority charge carriers of CoS, i.e. holes, localized in its VB (Figure 10). A major problem might arise from the eventual surface formation of CoI_2 with consequent alteration of the band properties of the iodide-modified CoS CE. The verification of the possible ex-

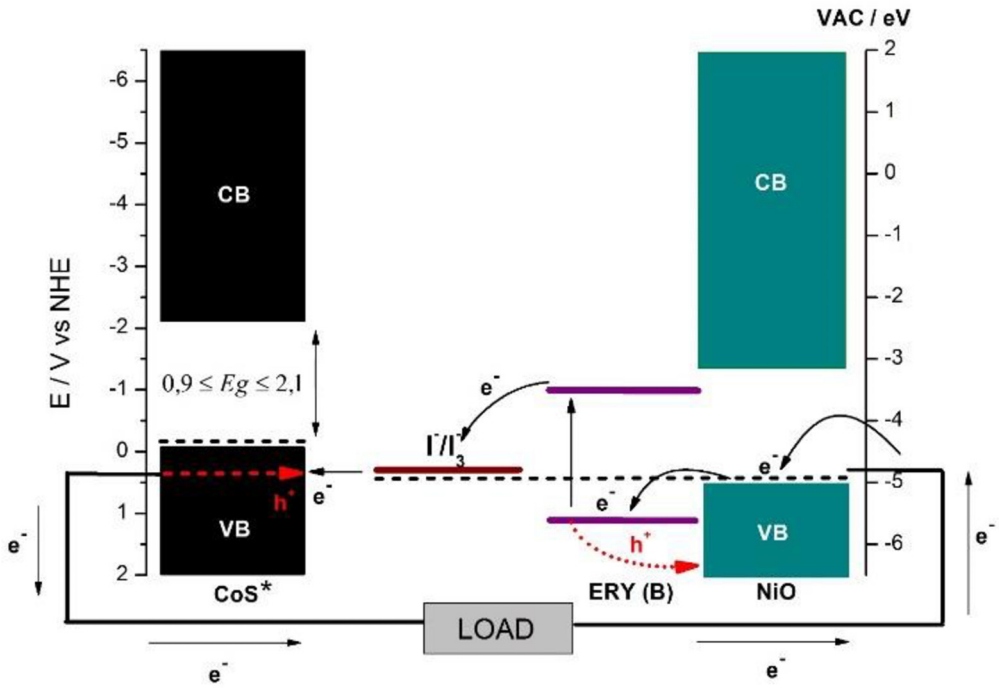

Figure 10. Schematic band representation of the functioning of the p-DSC with CoS CE. The light absorption by the photosensitizer Ery (B), promotes the electrons from the HOMO (-5,69 ev) to the LUMO (-3,63) level.[32] The electrons are transferred to the redox couple I^-/I_3^- (0,35 V vs NHE) and the hole, in the HOMO of the dye is transferred to the valence band of NiO. The reduced redox mediator (I^-) migrates to the CE and is regenerated at the interface between the electrolyte and CoS. The oxidation of $3I^-$ to I_3^- is promoted by the hole recombination in the VB of CoS.(*) The band structure of CoS was approximated by VB XPS measurements.[33]

istence of the iodide salt can be done in a successive study by means of the XPS analysis of the CE surface in contact with triiodide/iodide electrolyte in rest condition and after electrochemical cycling. At this juncture it is important to highlight that CoS is a suitable anodic material for *p*-DSCs despite the *p*-type nature of its electrical transport since the employment of this alternative material does not cause a considerable decrease of overall efficiency in the NiO based *p*-DSC (Figures 6,7 and Table 1).

Conclusions

In this paper it has been demonstrated for the first time that CoS thin films can be used successfully as anodic counter electrodes (CEs) of *p*-type dye-sensitized solar cells (*p*-DSC) based on photoelectrochemically active NiO despite the intrinsic *p*-type nature of CoS. *p*-DSCs employing CoS anodes showed similar values of overall efficiency, fill factor and short circuit current density in comparison to those obtained with the DSCs utilizing platinized FTO anodes, i.e. the benchmark anodic material of the *p*-DSCs. External quantum efficiency spectra of the respective *p*-DSCs did not differ in passing from CoS to platinized FTO when erythrosine B was the dye-sensitizer of NiO photocathode. The analysis of the impedance spectroscopy data for the two different types of *p*-DSCs differing for the nature of the CE was conducted adopting the equivalent circuit defined by Bisquert for *n*-type DSCs. The nature of the CEs affected the charge transport parameters as well as the charge carrier properties of NiO photocathode. It was found that the CE influences the charge transport properties of the photoactive cathode through the term of charge transfer resistance at the CE/electrolyte interface whereas the double layer capacitance of the CE/electrolyte interface affects the open circuit potential of the device as well as the lifetime of the photoinjected hole. CoS presented a higher value of interfacial charge transfer resistance with respect to platinized FTO, and a lower value of interfacial capacitance. The latter finding was in part ascribed to the eventual occurrence of anionic exchange at the sulphide surface with the iodide reactant. In conclusion, the present study supports the use of CoS as anodic material for p-DSC since CoS is much cheaper than platinized FTO but the corresponding photoelectrochemical performances are very similar. Further studies should be conducted in the near future to evaluate the efficiency and stability of CoS in variedly designed *p*-DSCs. The use of redox couples alternative to the mediator I_3^-/I^-, here considered, is particularly envisaged since it is expected to improve the efficiency and the stability of CoS counter electrodes also in a *p*-type device. In this respect, it has been previously recognized that CoS works very well as anode for the reversible oxidation of the reduced forms of redox shuttles like ferrocinium/ferrocene or the bipyridyl complexes of Co(III)/Co(II).[13] For the future work it is planned the use of a more performing dye, e.g. P1, for NiO based *p*-DSCs to evaluate whether how CoS CEs will sustain the more demanding conditions of higher photocurrents and larger photovoltages.

SUPPORTING INFORMATION SUMMARY

- Experimental
- Section S1: Spectral data
- Section S2: Calculation of the charge transport parameters in NiO porous layers

ACKNOWLEDGEMENTS

This work was supported by FAPESP (Fundação de Amparo à Pesquisa do Estado de São Paulo, proc: 2013/07396-7, 2013/25028-5 and 2008/57872-1) and CAPES (Coordenação de Aperfeiçoamento de Pessoal de Nível Superior), CAPES 024/2012 Pro-equipamentos. We especially thank Mr. Luiz Meneghetti Jr. for the technical support. Part of this search was financed by the the University of Rome "LA SAPIENZA" through the program Ateneo 2012 (Protocol No. C26 A124AXX) and by Regione Lazio and CHOSE. A.D.C. and D.D. Acknowledge also the financial support from MIUR through the research project PRIN 2010–2011 (protocol no. 20104XET32).

Keywords: Cobalt sulfide · Counter electrode · Dye Sensitized Solar Cells · P-type solar cell · solar energy

[1] S. Mathew, A. Yella, P. Gao, R. Humphry-Baker, C. F. E. , N. Ashari-Astani, I. Tavernelli, U. Rothlisberger, N. Khaja, M. Grätzel, *Nat Chem* **2014**, *6*, 242–247.
[2] B. O'regan, M. Gräzel, *Nature* **1991**, *353*, 737–740.
[3] E. Galoppini, J. Rochford, H. Chen, G. Saraf, Y. Lu, A. Hagfeldt, G. Boschloo, *J. Phys. Chem. B* **2006**, *110*, 16159–16161.
[4] D. Dini, Y. Halpin, J. G. Vos, E. A. Gibson, *Coord. Chem. Rev.* **2015**, *304–305*, 179–201.
[5] S. Thomas, T. G. Deepak, G. S. Anjusree, T. A. Arun, S. V. Nair, A. S. Nair, *J. Mater. Chem. A* **2014**, *2*, 4474.
[6] J.-L. Lan, Y.-Y. Wang, C.-C. Wan, T.-C. Wei, H.-P. Feng, C. Peng, H.-P. Cheng, Y.-H. Chang, W.-C. Hsu, *Curr. Appl. Phys.* **2010**, *10*, S168–S171.
[7] N. Fu, X. Xiao, X. Zhou, J. Zhang, Y. Lin, *J. Phys. Chem. C* **2012**, *116*, 2850–2857.
[8] H. Wang, Y. H. Hu, *Energy Environ. Sci.* **2012**, *5*, 8182.
[9] I. Ahmad, J. E. McCarthy, M. Bari, Y. K. Gun'ko, *Sol. Energy* **2014**, *102*, 152–161.
[10] B. Park, M. Pazoki, K. Aitola, S. Jeong, E. M. J. Johansson, A. Hagfeldt, G. Boschloo, *ACS Appl. Mater. Interfaces* **2014**, *6*, 2074–9.
[11] M. Wang, A. M. Anghel, B. Marsan, N.-L. Cevey Ha, N. Pootrakulchote, S. M. Zakeeruddin, M. Grätzel, *J. Am. Chem. Soc.* **2009**, *131*, 15976–15977.
[12] M. Congiu, L. G. S. Albano, F. Decker, C. F. O. Graeff, *Electrochim. Acta* **2015**, *151*, 517–524.
[13] M. Congiu, A. Lanuti, A. di Carlo, C. F. O. Graeff, *Sol. Energy* **2015**, *122*, 87–96.
[14] J. Yang, C. Bao, K. Zhu, T. Yu, F. Li, J. Liu, Z. Li, Z. Zou, *Chem. Commun.* **2014**.
[15] M. S. Faber, K. Park, M. Cabán-Acevedo, P. K. Santra, S. Jin, *J. Phys. Chem. Lett.* **2013**, *4*, 1843–1849.
[16] M. Congiu, O. Nunes-Neto, M. L. De Marco, D. Dini, C. F. O. Graeff, *Thin Solid Films* **2016**, *612*, 22–28.
[17] J.-Y. Lin, J.-H. Liao, T.-C. Wei, *Electrochem. Solid-State Lett.* **2011**, *14*, D41–D44.
[18] J. Huo, M. Zheng, Y. Tu, J. Wu, L. Hu, S. Dai, *Electrochim. Acta* **2015**, *159*, 166–173.
[19] S. SrinivasaRao, C. V. V. M. Gopi, S.-K. Kim, M.-K. Son, M.-S. Jeong, A. D. Savariraj, K. Prabakar, H.-J. Kim, *Electrochim. Acta* **2014**.
[20] A. Bard, L. Faulkner, *Electrochemical Methods: Fundamentals and Applications*, **2001**.
[21] E. a Gibson, M. Awais, D. Dini, D. P. Dowling, M. T. Pryce, J. G. Vos, G. Boschloo, A. Hagfeldt, *Pccp* **2013**, *15*, 2411–20.
[22] M. Awais, E. Gibson, J. G. Vos, D. P. Dowling, A. Hagfeldt, D. Dini, *ChemElectroChem* **2014**, *1*, 384–391.
[23] A. J. Bard, L. R. Faulkner, *Electrochem. Methods, 2nd ed.; Wiley New York* **2001**, 31.
[24] D. Pumiglia, M. Giustini, D. Dini, F. Decker, A. Lanuti, S. Mastroianni, S. Veyres, F. Caprioli, *ChemElectroChem* **2014**, *1*, 1388–1394.
[25] S. Mastroianni, A. Lembo, T. M. Brown, A. Reale, A. Di Carlo, *Chemphyschem* **2012**, *13*, 2964–75.
[26] A. Agresti, S. Pescetelli, A. Quatela, S. Mastroianni, T. M. Brown, A. Reale, C. A. Bignozzi, S. Caramori, A. Di Carlo, *RSC Adv.* **2014**, *4*, 12366.
[27] S. Sheehan, G. Naponiello, F. Odobel, D. P. Dowling, A. Di Carlo, D. Dini, *J. Solid State Electrochem.* **2015**, *19*, 975–986.
[28] F. De Rossi, L. Di Gaspare, A. Reale, A. Di Carlo, T. M. Brown, *J. Mater. Chem. A* **2013**, *1*, 12941.
[29] F. Fabregat-Santiago, J. Bisquert, E. Palomares, L. Otero, D. Kuang, S. M. Zakeeruddin, M. Gratzel, *J. Phys. Chem. C* **2007**, *111*, 6550–6560.
[30] B. Hirschorn, M. E. Orazem, B. Tribollet, V. Vivier, I. Frateur, M. Musiani, *Electrochim. Acta* **2010**, *55*, 6218–6227.
[31] F. Fabregat-Santiago, G. Garcia-Belmonte, I. Mora-Seró, J. Bisquert, *Phys. Chem. Chem. Phys.* **2011**, *13*, 9083.
[32] A. Nattestad, M. Ferguson, R. Kerr, Y.-B. Cheng, U. Bach, *Nanotechnology* **2008**, *19*, 295304.
[33] A. Galtayries, S. Wisniewski, J. Grimblot, *J. Electron Spectros. Relat. Phenomena* **1997**, *87*, 31–44.

Submitted: April 1, 2016
Accepted: June 28, 2016